The Effect of a Secondary Process on Polymer Crystallization Kinetics – 3. Co-poly (lactic acid)

Abdul Aziz, Azizan; Samsudin, Sani; Hay, James; Jenkins, Michael

DOI:
10.1016/j.eurpolymj.2017.07.006

Document Version
Peer reviewed version

Citation for published version (Harvard):
Abdul Aziz, A, Samsudin, S, Hay, J & Jenkins, M 2017, 'The Effect of a Secondary Process on Polymer Crystallization Kinetics – 3. Co-poly (lactic acid)', *European Polymer Journal*, vol. 94, pp. 311-321. https://doi.org/10.1016/j.eurpolymj.2017.07.006

The Effect of a Secondary Process on Polymer Crystallization Kinetics – 3.

Co-poly (lactic acid)

Azizan A Aziz, Sani A. Samsudin[1], James N. Hay* and Michael J. Jenkins,

The School of Metallurgy and Materials,

College of Physical Science and Engineering,

The University of Birmingham,

Edgbaston,

Birmingham B15 2TT, UK

[1]Dr. Sani A Samsudin
Department of Bioprocessing and Polymer Engineering
Faculty of Chemical and Energy Engineering
Universiti Teknologi Malaysia
81310 UTM Skudai
Johor, Malaysia
Email: saniamril@utm.my

Figures: - 11.

Micrographs: -2

Tables: - 3.

*Corresponding Author
Tel: +44 121 414 4544 Fax: +44 121 414 5232
E-mail address: j.n.hay@bham.ac.uk

The Effect of a Secondary Process on Crystallization Kinetics – 3.

Co-poly (lactic acid),

by

Azizan A Aziz, Sani A. Samsudin[1], James N. Hay* and Michael J. Jenkins,

The School of Metallurgy and Materials, College of Physical Science and Engineering,

The University of Birmingham, Edgbaston, Birmingham B15 2TT,UK.

Abstract.

The crystallization kinetics of a copolymer of L-lactic acid with 4% D-lactic acid has been studied using FTIR spectroscopy by measuring the absorbance of the crystalline carbonyl stretching band at 1759 cm^{-1}. Copolymerization greatly reduced the rate of crystallization and the technique directly measured the relative crystallinity over extended periods with sufficient accuracy to test the validity of the Avrami equation. This was modified to account for the simultaneous presence of a secondary process from the onset of crystallization, such that the overall fractional crystallinity, X_t, is related to the lapsed time, t, by

$$X_t = X_{p,\infty}\,(1 - \exp -Z_p t^n)(1 + k_s t^{\frac{1}{2}})$$

where $X_{p,\infty}$ is the final fractional crystallinity achieved by the primary process, Z_p is the primary composite rate constant incorporating nucleation and growth, and k_s is the secondary rate constant.

The additional crystallinity produced by the secondary processes is sufficient to account for the observed fractional constant n values on analysis of the total development of crystallinity with time. It was concluded that the analysis using the Avrami equation should be restricted to the time dependence of the crystallinity produced by the primary process alone.

Keywords: Copoly (lactic acid); crystallization kinetics; primary and secondary crystallization; concurrent processes.

1 Introduction

There is increasing commercial interest in poly (L-lactic acid), PLA, as an environmentally-friendly thermoplastic replacement for oil based polyolefins since it is produced from renewable sources, is biodegradable and biocompatible [1-3]. As a partially crystalline polymer it has thermal and mechanical properties comparable to those of the polyolefins but as an amorphous polymer the glass transition temperature is somewhat low, 55 ^{o}C, leading to physical ageing altering the material properties with time at room temperature and in vitro.

The crystallization behaviour of PLA in bulk and from solution has been extensively studied using a wide range of techniques, light microscopy, DSC, X-ray crystallography and FTIR spectroscopy, to control the crystallinity and rate of crystallization [4-10]. In this respect, fruitful areas of research have been in controlling the stereoregularity of PLA by copolymerization with D-lactic acid and D- and meso-lactides [11,12] which greatly reduced the rate of crystallization while the addition of talc [12] and other minerals [13,14] greatly increase the rate of crystallization by acting as nucleating agents.

However, in analyzing the crystallization kinetics with the Avrami equation [15] most authors, [11-14] obtained constant fractional n values between 2.5 and 3.5. Fractional values have no mechanistic significance in terms of the crystallization mechanisms adopted by Avrami, i.e.,

$$X_t = X_\infty (1 - \exp - Zt^n) \qquad 1.$$

where X_t is the fractional crystallinity which has developed at time t, X_∞ is the limiting fractional crystallinity finally achieved, Z is a composite rate constant incorporation nucleation rate or density and growth rate; n is an integer constant characteristic of the crystallization mechanism and in terms of the crystallization models of linear growth of crystals in 1,2 and 3 dimensions and heterogeneous (constant nucleation density) or

homogeneous nucleation (constant nucleation rate) adopted by Avrami n should have integral values between 1 and 4.

Similar results have been obtained with many other polymers but recently in a study of the crystallization kinetics of polyesters, in particular poly (ethylene terephthalate) [16-18] and poly (ϵ-caprolactone) [19, 20], the fractional n values have been explained in terms of an overlap between primary and secondary crystallizations; the additional crystallinity due to the secondary process increased the observed n value to above that attributed to the crystallization mechanism in proportion to the value of the secondary rate constant.

In order to extend these kinetic studies and test the generality of these observations the isothermal crystallization of a copolymer of PLLA with 4% D-lactic acid has been studied using FTIR spectroscopy thermal analysis. This technique has the potential to measure the development of crystallinity for extended periods and with sufficient accuracy to separate primary and secondary processes. In this way it is hoped to explain the frequently observed fractional n values in the analysis of the crystallization kinetics of polymers and extend the explanation to another polymer system.

2.0 Experimental

A random copolymer of L-lactic acid with 4% D-lactic acid, co-PLA, from NatureWorks LLC, USA was used in this study. It was supplied as semi-crystalline moulding pellets with a molecular weight of 194 kg mol^{-1}. Thin films, 10-15 μm thick, were prepared by evaporation of 5% w/v solution in chloroform and solvent removed by storing overnight in a heated vacuum oven at 80 ^{o}C.

These films were mounted vertically between two 100 mg KBr discs (approx. 1mm thick) in a Linkam THM 600 hot-stage cell and placed within the sample chamber of a Nicolet FTIR spectrometer, model Magna IR 8700 equipped with a DTGS-KBr detector and controlled by Omnic 8.1 software. Spectra of co-PLA were measured in transmission at a resolution of 1-4

cm^{-1} and total of a 100 scans were accumulated for each spectrum along with a background spectrum (a blank 200 mg KBr disc was used in measuring the background spectrum). Automatic smoothing and baseline corrections were made before analyzing the spectra.

In the crystallization experiments, the samples were heated to the melt at a heating rate of 50 $^oC\ min^{-1}$and held at 200 ^oC for 2 minutes to ensure the sample was completely melted and to erase thermal history. It was then immediately cooled to the isothermal crystallization temperature. A series of spectra were collected at a constant time interval of 2 min over 1000-1500 min.

3.0 Results and Discussion

3.1 Primary Crystallization

The IR spectrum of PLA has been well characterized especially the changes which occur on crystallization. It has been reported, [9, 21-24] that the most significant change is to the broad intense carbonyl stretching band, centred at 1755 cm^{-1}; it changes in shape on crystallization, see Fig. 1, narrowing by losing intensity between 1740-1750 and1765 -1780 cm^{-1} as well as increasing in intensity with a shift in λ_{max} from 1749 to 1759 cm^{-1}. These changes are reversed on melting. The change in shape of the carbonyl bands is due to the presence of chain conformers which are present in equilibrium in the mobile liquid state but change on crystallization corresponding to the formation of 10:3 helix.

The breadth of the carbonyl band has been attributed to the presence of four overlapping peaks [24] assigned to different conformations of the carbonyl group and in particular the band with λ_{max} at 1759 cm^{-1} has been assigned to the *gt* conformer. This is adopted by the segments in the crystalline regions but is also present in the amorphous regions in thermal equilibrium with other conformers. In isothermal measurements the change in absorbance at 1759 cm^{-1} is attributed to the increase in crystallinity.

The change in absorbance at 1759 cm^{-1}on crystallization was analyzed as follows; the initial absorbance, A_o, before crystallization had started, was attributed to the amorphous content. Assuming a two component system for the partially crystalline copolymer, the absorbance at time t, A_t, has amorphous and crystalline components such that,

$$A_t = (1 - X_t)A_o + X_t A_c \qquad 2.$$

where A_c is the absorbance of a totally crystalline sample of constant thickness. The fractional crystallinity, X_t, is

$$X_t = \frac{(A_t - A_o)}{(A_c - A_o)} \qquad 3.$$

Since A_c is not normally measured, a relative crystallinity, X, relative to that achieved at the end of the measurements was defined as

$$X = \frac{X_t}{X_\infty} = (A_t - A_o) \Big/ (A_\infty - A_o) \qquad 4.$$

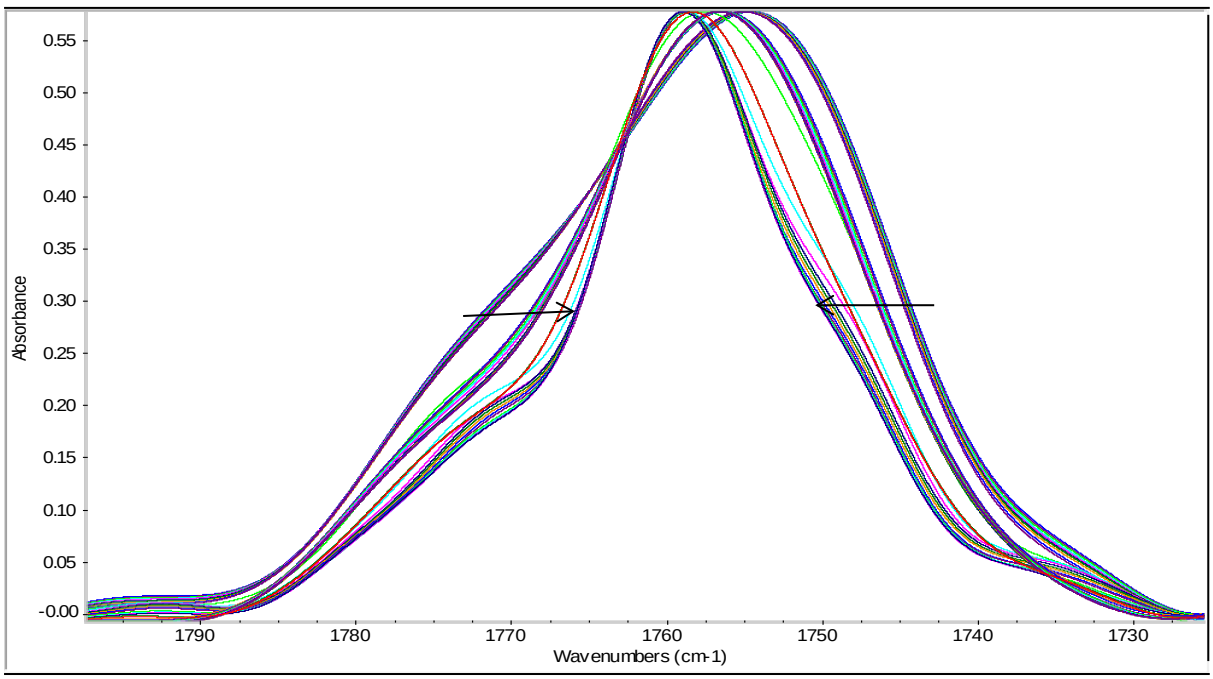

Fig. 1. The change in shape of the carbonyl band on crystallization at 120 ^oC.

(Arrows indicate the direction of increasing crystallinity).

The increase in relative crystallinity with time over the temperature range 124-136 ^{o}C is shown in Fig. 2 where the point to point variation in relative crystallinity is shown with time; initially this increased exponentially with time but is followed by a linear increase with the logarithm of time over the final stage of the crystallization. This later stage is attributed to a secondary process and has conventionally been separated from the primary by their different time dependences.

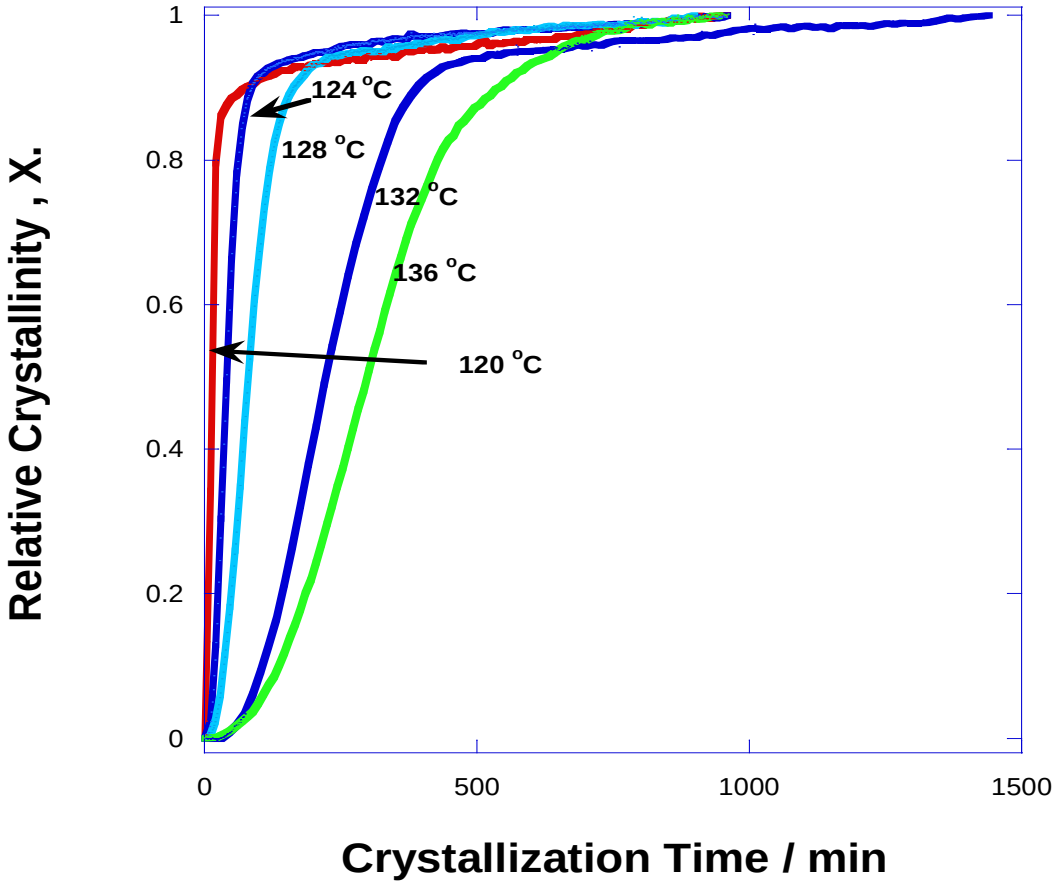

Fig. 2. The increase in relative crystallinity, X, with time.

The primary process is attributed to the nucleation and growth of lamellar crystals which by branching developed into spherical particles, or spherulites. For the growth and impingement

of spherical particles, this should follow an Avrami equation with n=3.0 or 4.0 depending on the type of primary nucleation, homogeneous or heterogeneous respectively [13]. It can be seen in Fig. 2 that the half-lives of the crystallization increased with crystallization temperature. The time dependence over the initial part of the crystallization was analyzed using the Avrami equation, assuming that it ended before the onset of secondary crystallization at $X_{p,\infty}$, i.e.

$$X_{p,t} = X_{p,\infty}(1 - \exp(-Z_p\, t^n)) \qquad 5.$$

where Z_p and n are the same as in eq.1 for the primary process alone. It follows that

$$\log(-\ln\left(1 - \left(X_{p,t}/X_{p,\infty}\right)\right)) = n \log t + \log(Z_p) \qquad 6.$$

Plots of $\log(-\ln(1-(X_{p,t}/X_{p,\infty})))$ against log (t) were linear between 0.01 and 0.95 relative crystallinity, see Fig. 3. In this analysis $X_{p,\infty}$ was used as an adjustable parameter in the region in which the time dependence of X_p was observed to change and the value chosen from the best linear fit of the data to eq. 6 as determined by R^2, see Figs. 3, 4 and 5. The value of n and log (Z_p) were determined from the slope and intercept at t=1.0 for this value of $X_{p,\infty}$ and over 1-95% conversion . The analysis of the time dependence of the primary crystallization is summarized in Fig. 5 over the temperature range studied and the Avrami rate parameters are listed in Table 1. In every case, the n value was fractional, 2.5 ± 0.4, and as such was inconsistent with the growth of 3-dimensional spherulites for which a value of 3.0 or 4.0 would be expected, depending on primary nucleation being heterogeneous or homogeneous respectively.

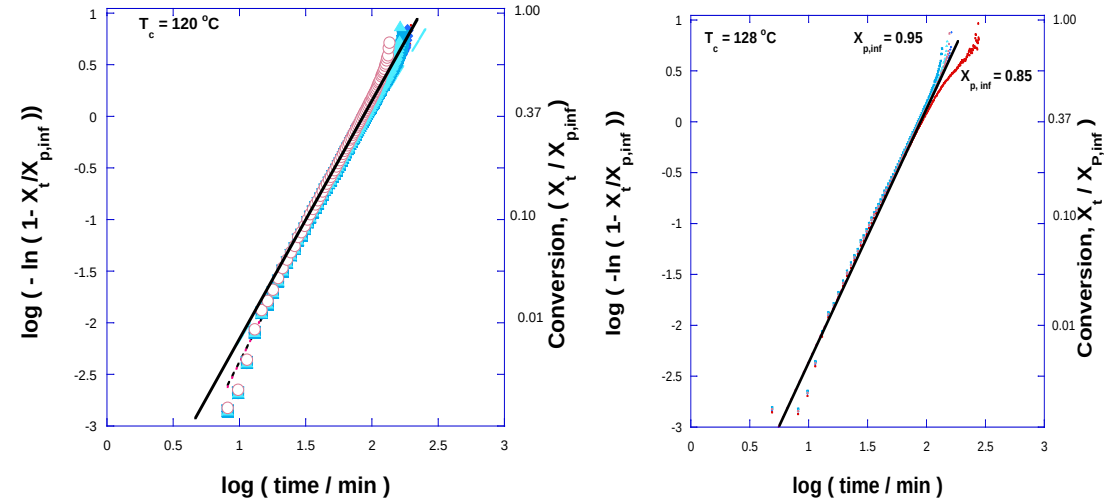

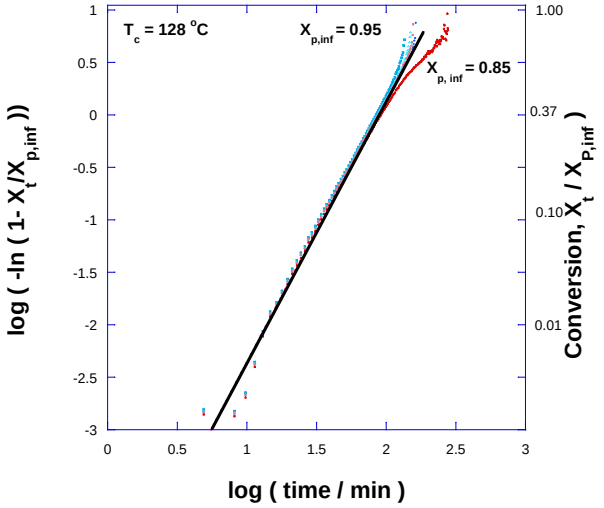

Fig. 3. Double log plots of log(-ln(1-($X_p/X_{p,\infty}$))) against log (t)
The effect of changing $X_{p,\infty}$.

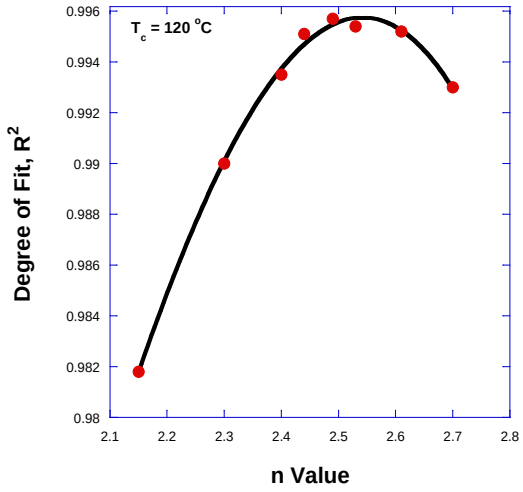

Fig. 4. The effect of changing $X_{p,\infty}$ on the degree of fit.

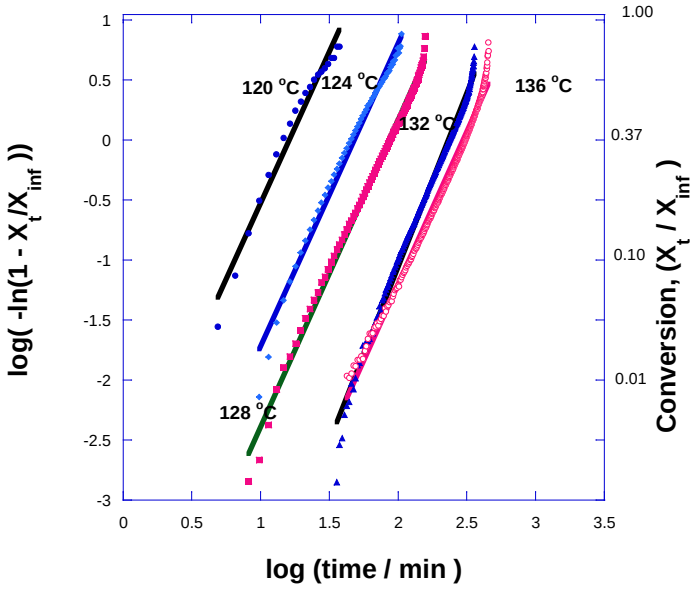

Fig. 5. Summary of the Avrami analysis over temperature range studied.

Table 1. Primary Crystallization Rate Parameters.

Crystallization Temperature/ ^{o}C	**120**	**124**	**128**	**132**	**136**
n Value ± 0.2	**2.5**	**2.5**	**2.5**	**2.8**	**2.1**
-log (Z_p / min^{-n})	**3.06**	**4.24**	**4.87**	**6.87**	**6.30**
Relative crystallinity $X_{p,\infty}$	**0.91**	**0.92**	**0.89**	**0.94**	**0.83**
Variance R^2	**0.996**	**0.986**	**0.994**	**0.993**	**0.983**

3.2 The secondary process.

The secondary crystallization has previously been attributed to the thickening of the lamellae by secondary nucleation on the fold surface and growth perpendicular to length of the lamellae [16-20] which was considered to be diffusion controlled. The lamellar thickness increased linearly with the square root of the lapsed time, and was considered to occur as soon as the lamellae were produced by the primary process, such that the increased crystallinity due to secondary crystallization is

$$X_{p,t} = X_{p,t}\, k_s t^{1/2} \qquad 7.$$

The total crystallinity due to primary and secondary crystallization is accordingly

$$X_t = X_{p,t} + X_{s,t} \qquad 8.$$

$$X_t = X_{p,\infty}\,(1 - \exp(-Z_p t^n)(1 + k_s t^n) \qquad 9.$$

Once the primary process is complete, $X_{p,t} = X_{p,\infty}$, $\exp(-Z_p t^n) = 0$ and X_t will be a linear function of $t^{1/2}$ with slope k_s and intercept $X_{p,\infty}$ since

$$X_t = X_{p,\infty}(1 + k_s t^{\frac{1}{2}}) \qquad 10.$$

This dependence is shown in Fig. 6 and the rate parameters determined from it are listed in Table 2. The values determined for $X_{p,\infty}$ agreed closely with those determined by the best fit

11.

of the Avrami equation as listed in Table 1. Although the rate constants did not vary they tended to increase with temperature. This is inconsistent with nucleation controlled process but consistent with diffusion control.

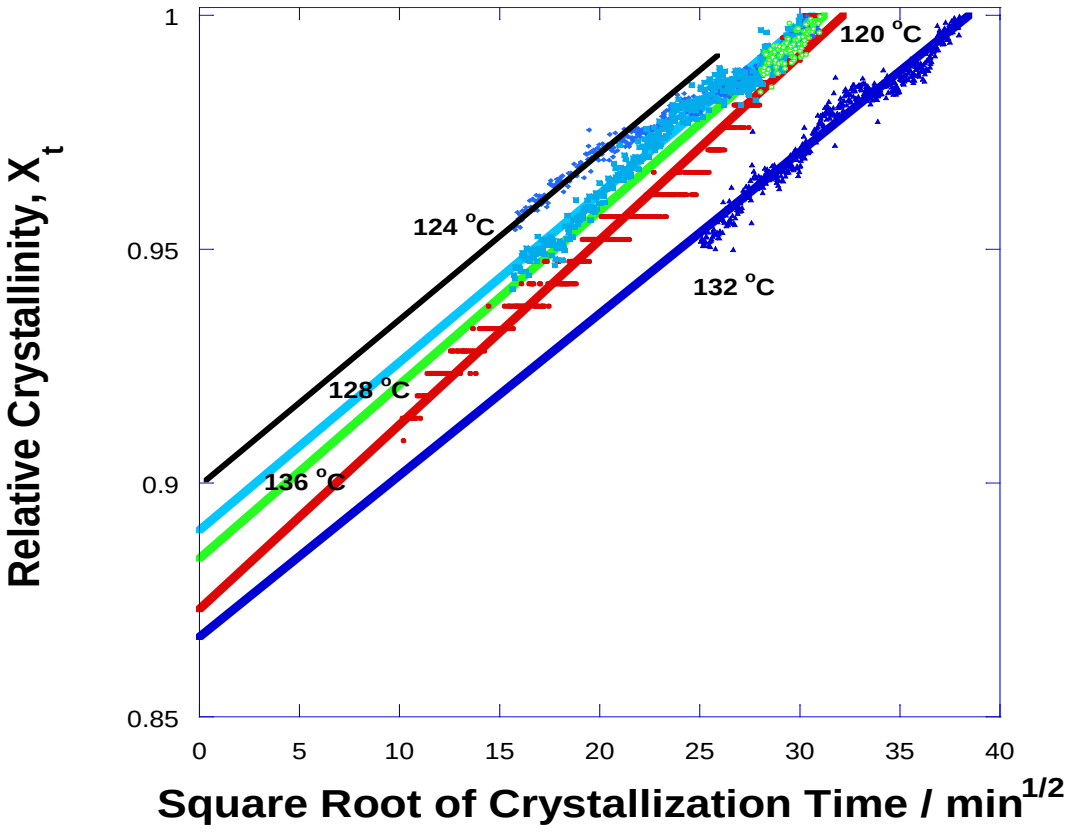

Fig. 6. The dependence of the extent of secondary crystallization on the square root of the lapsed time.

Table 2 Secondary Crystallization Rate Parameters.

Crystallization Temperature / °C					

	120	124	128	132	136
Secondary Rate Constant, ks / $min^{-1/2}$ ± 0.0005	**0.0031**	**0.0030**	**0.0041**	**0.0040**	**0.0042**
$X_{p,\infty}$	**0.87**	**0.92**	**0.89**	**0.87**	**0.83**

3.3 The fit of Crystallization data to equation 9.

Eq. 9 was derived assuming that only the primary process obeyed an Avrami rate equation. Accordingly

$$X_{p,t} = X_{p,\infty}\left(1 - \exp - Z_p t^n\right) = {X_t}/{\left(1 + k_s\, t^{\frac{1}{2}}\right)} \qquad 10.$$

$$(1 - X_t)/\left\{X_{p,\infty}\left(1 + k_s t^{\frac{1}{2}}\right)\right\} = \exp(-Z_p\ t^{1/2}) \qquad 11.$$

$$\text{And}\quad \log(-\ln\{1 - X_t\}/[X_{p,\infty}\left(1 + k_s t^{\frac{1}{2}}\right)]\}) = \log(Z_p) + n\log(t) \qquad 12.$$

A plot of log (-ln (1- X_t /{ $X_{p,\infty}$ (1+ $k_s t^{1/2}$)})) against log (t) should be linear with a slope of n. Fig. 7 is a plot of the crystallization data obtained at 136 ^{o}C, and for which the slope, from 0.01 to 0.99 conversion, is 1.99 ± 0.10. The Avrami rate parameters for the primary crystallization determined by this method are shown in Table 3 and every case n was 2.0 ± 0.1 with a greatly reduced scatter than observed in Fig. 3. The value of n was consistent with the growth of spherulites confined to grow in 2-dimensions; that is discs confined to the thickness of the thin films and nucleated by heterogeneous nuclei.

In order to confirm that eq. 9 was a valid description of the crystallization-time dependence the relative crystallinity was calculated at each temperature using the rate parameters listed in Tables 2 and 3. A comparison was made between the experimental and calculated data to shown that the equation was a reasonable fit of the overall time dependence of the crystallizations in Fig. 8. Small variations were observed between calculated and observed 13.

relative crystallinity-time dependences. However, to highlight the differences between the two curves, the calculated crystallinity was subtracted from the experimental and the difference plotted against time in Fig. 9. The maximum difference observed was about 0.02 for most of the crystallizations, excepting that obtained at 124 ^{o}C which exceeded 0.04. Nevertheless the data compared favorably with the accuracy in measuring the absorbance of ±0.010.

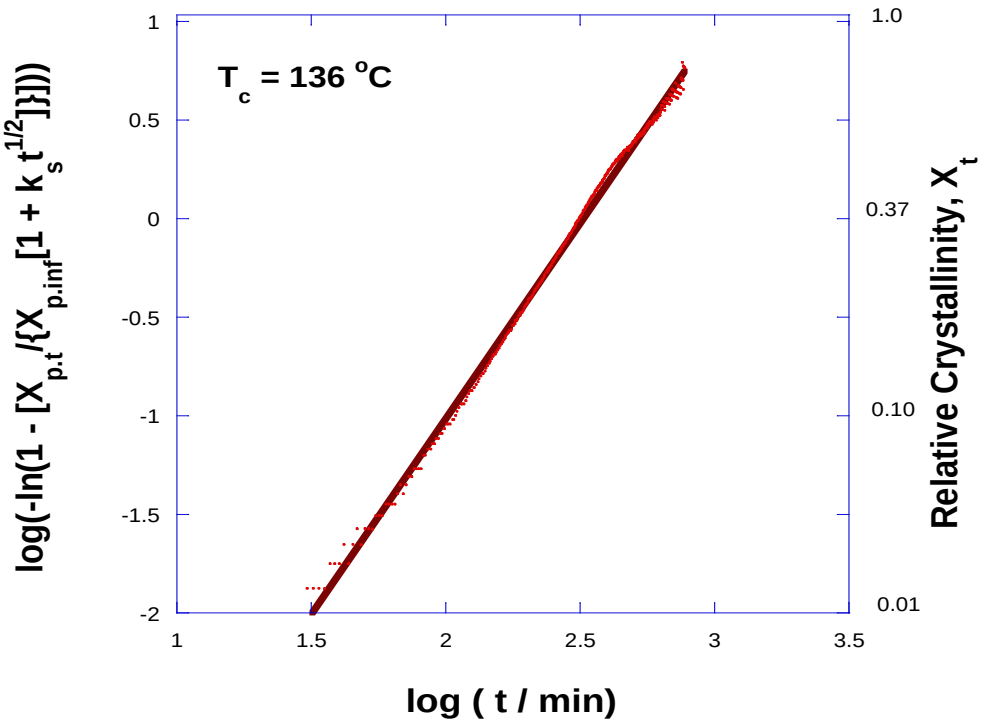

Fig. 7. Analysis of the primary crystallization using equation 9.

Table 3 The Primary Crystallization Rate Parameters.

Crystallization Temperature / °C	120	124	128	132	136
$X_{p,\infty}$	0.87	0.92	0.89	0.87	0.83
Half-life / min	12	38	75	205	280
n Value ± 0.10	2.00	2.00	2.00	2.20	1.99
Z / min^{-2} x 10^6	4440	479	123	15.7	8.84

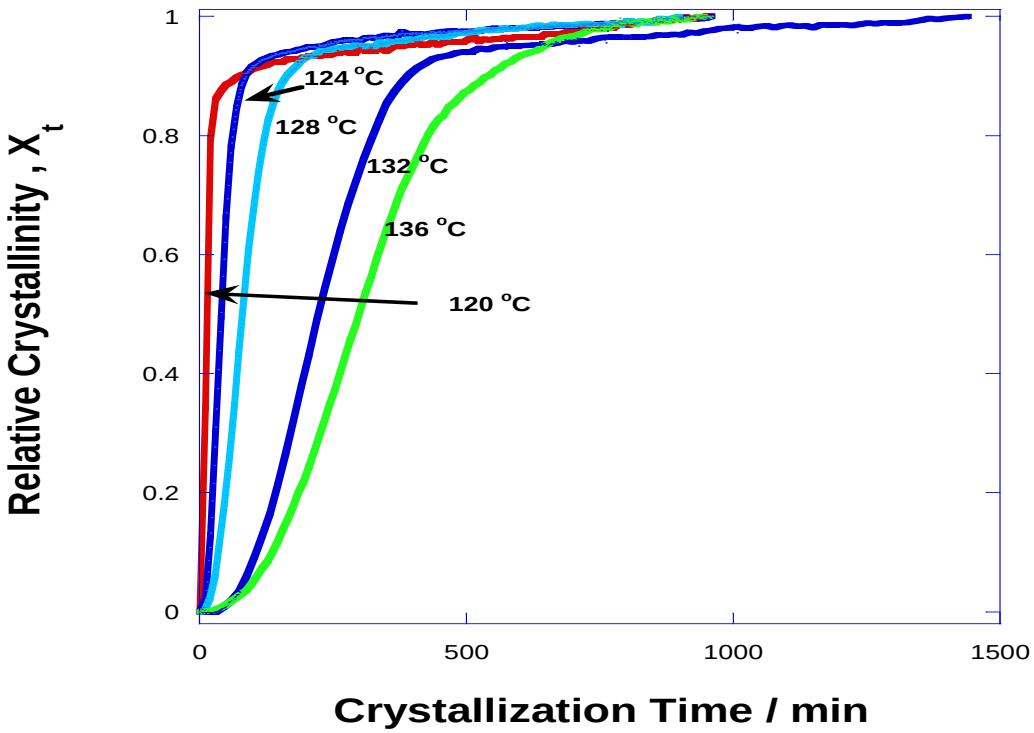

Fig. 8. Calculated (dots) and experimental (lines) relative crystallinity against time.

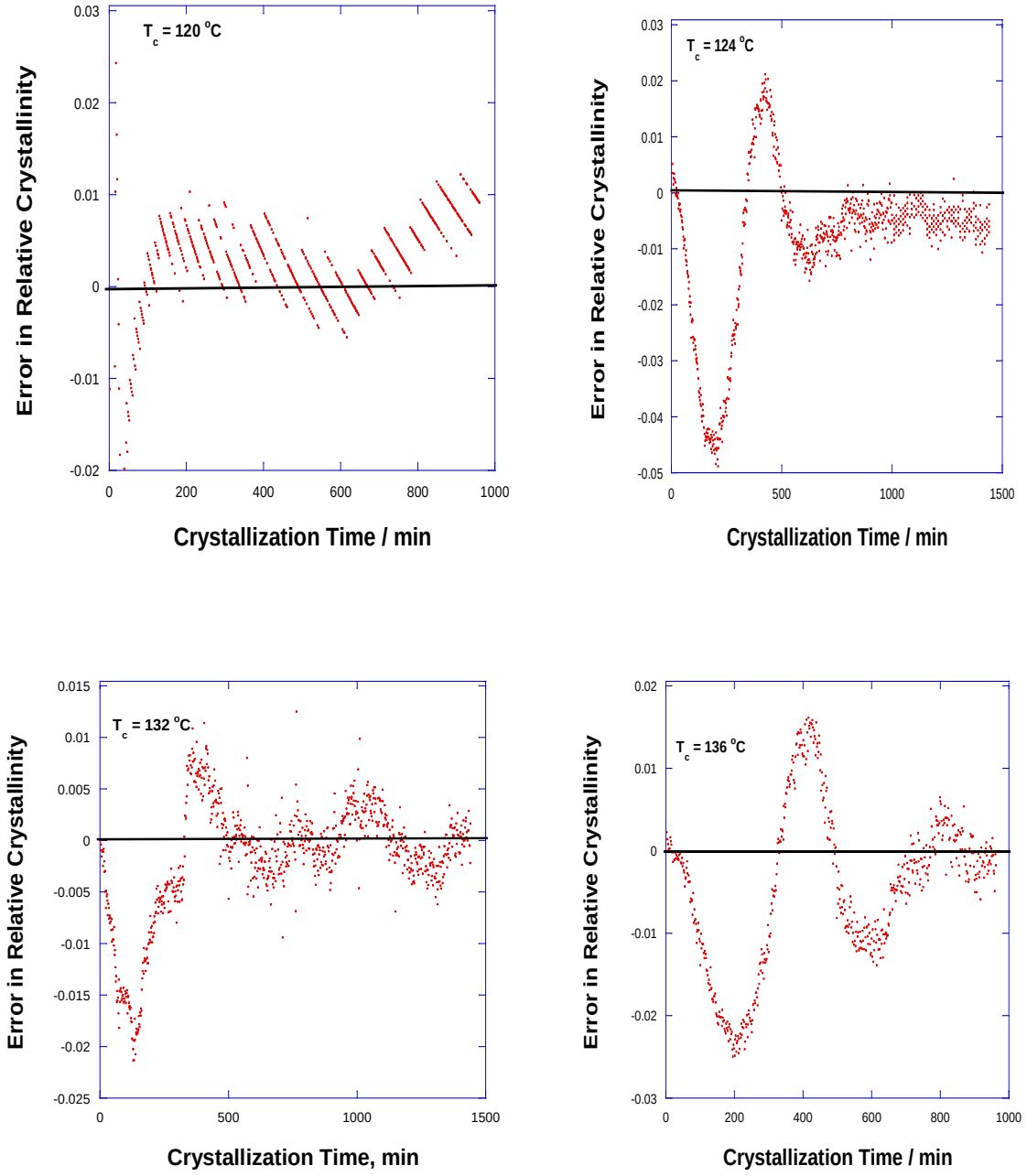

Fig. 9. The error in fitting equation 9 to experimental data at various crystallization temperatures.

The relative amounts the individual components of primary, $X_{p,t}$, and secondary crystallinities, $X_{s,t}$ contributed to the overall relative crystallinity was also calculated from the rate parameters listed in Tables 2 and 3 are shown in Figs. 10 and 11. By comparison it can be seen that secondary crystallization makes a substantial contribution to the overall crystallinity in the early stages and accounts for all of the increase in the final stages. The upward curvature of the initial part of the secondary crystallization –time dependence is attributed to the exponential shape of the primary crystallization dependence which makes an increasing contribution with time until the primary process ceases. After that the increase is due to the dependence on the square root of time. In analyzing the initial stages of the crystallization without correcting for the presence of secondary process an increased value of n over that required by the Avrami equation would be expected.

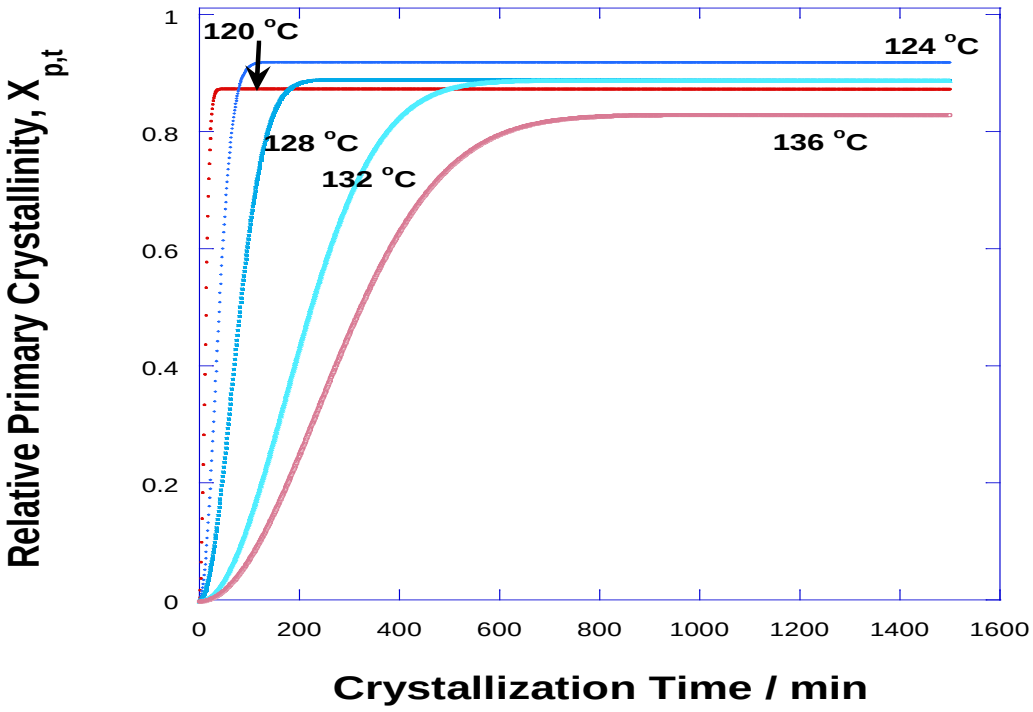

Fig. 10. The contribution of primary crystallization to the overall relative crystallinity

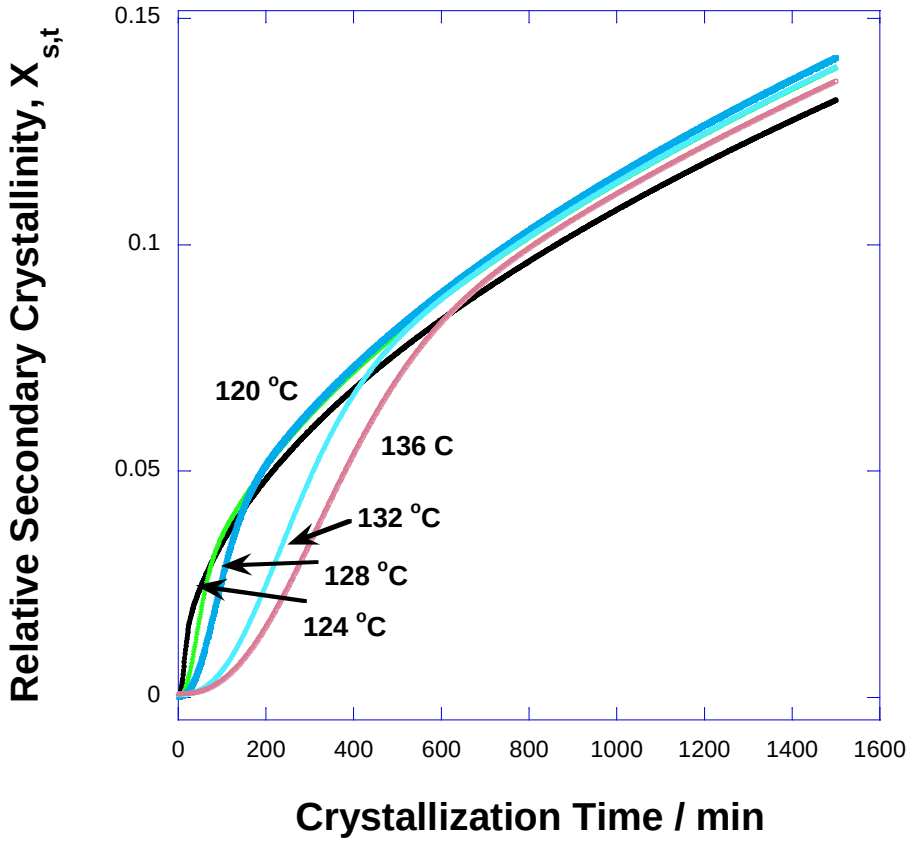

Fig. 11. The contribution of secondary crystallization to the overall relative crystallinity.

4.0 Conclusions

The absorbance of the carbonyl stretching band at 1759 cm^{-1} is a relative measure of the crystallinity of co-PLA and is sufficiently accurate to measure the kinetics of the conversion for extended periods. However, because of the breadth of the amorphous band it was not possible to separately determine amorphous and crystalline bands and the fractional crystallinity could not be determined without measuring it by some other means, e.g. from the heat of fusion. Both primary and secondary crystallizations have been measured over 1000-1500 min which allowed detailed analyses of their time dependence over an extended period. Primary crystallization exhibited an exponential dependence on time following an Avrami 18.

equation with n=2.0 with a half-life which increased with increasing temperature. This was consistent with nucleation control of the growth of spherulites which were confined by the film thickness to 2-dimensions.

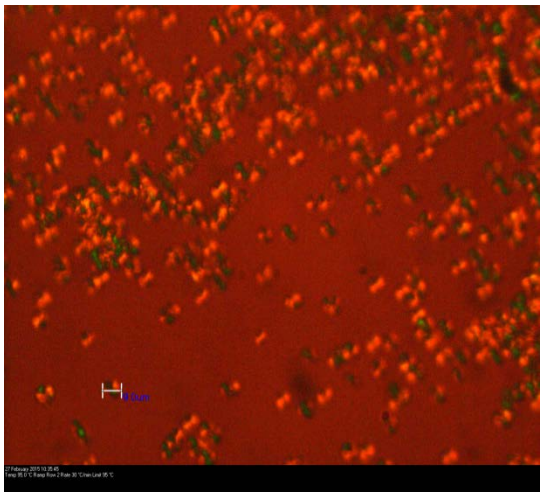

95 ^{o}C

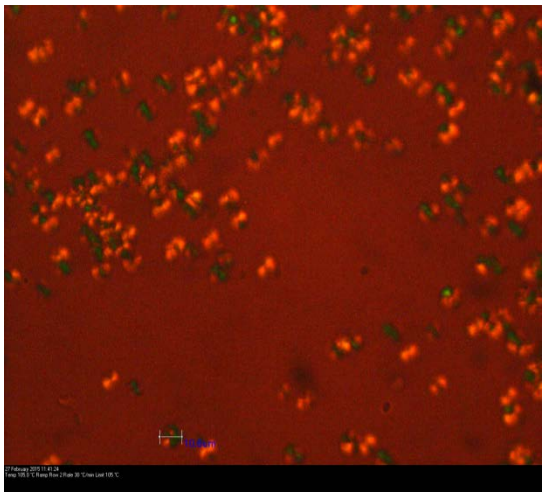

105 ^{o}C

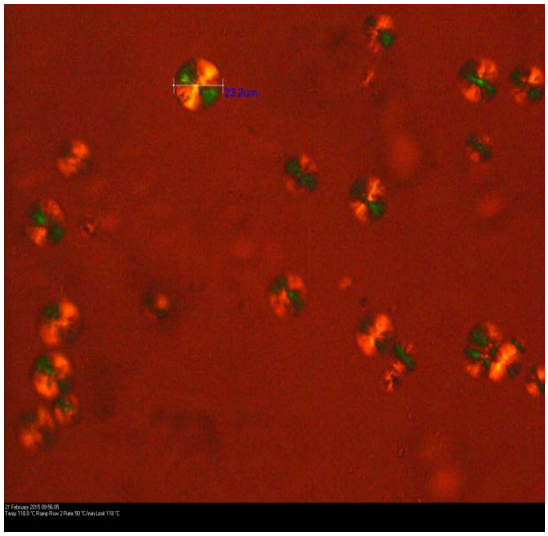

118 ^{o}C

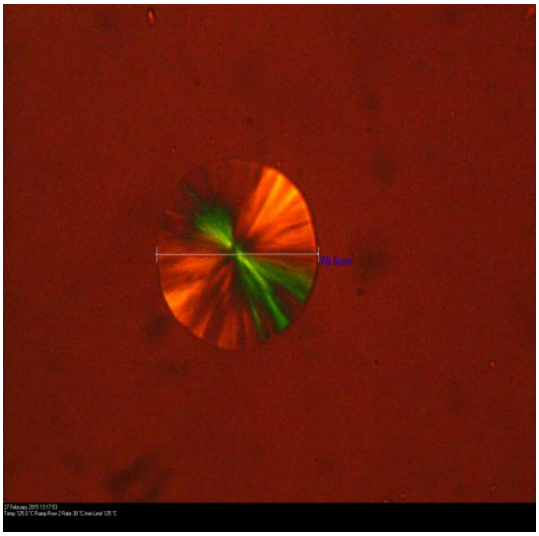

125 ^{o}C

Plate 1. Effect of crystallization temperature on nucleation density.

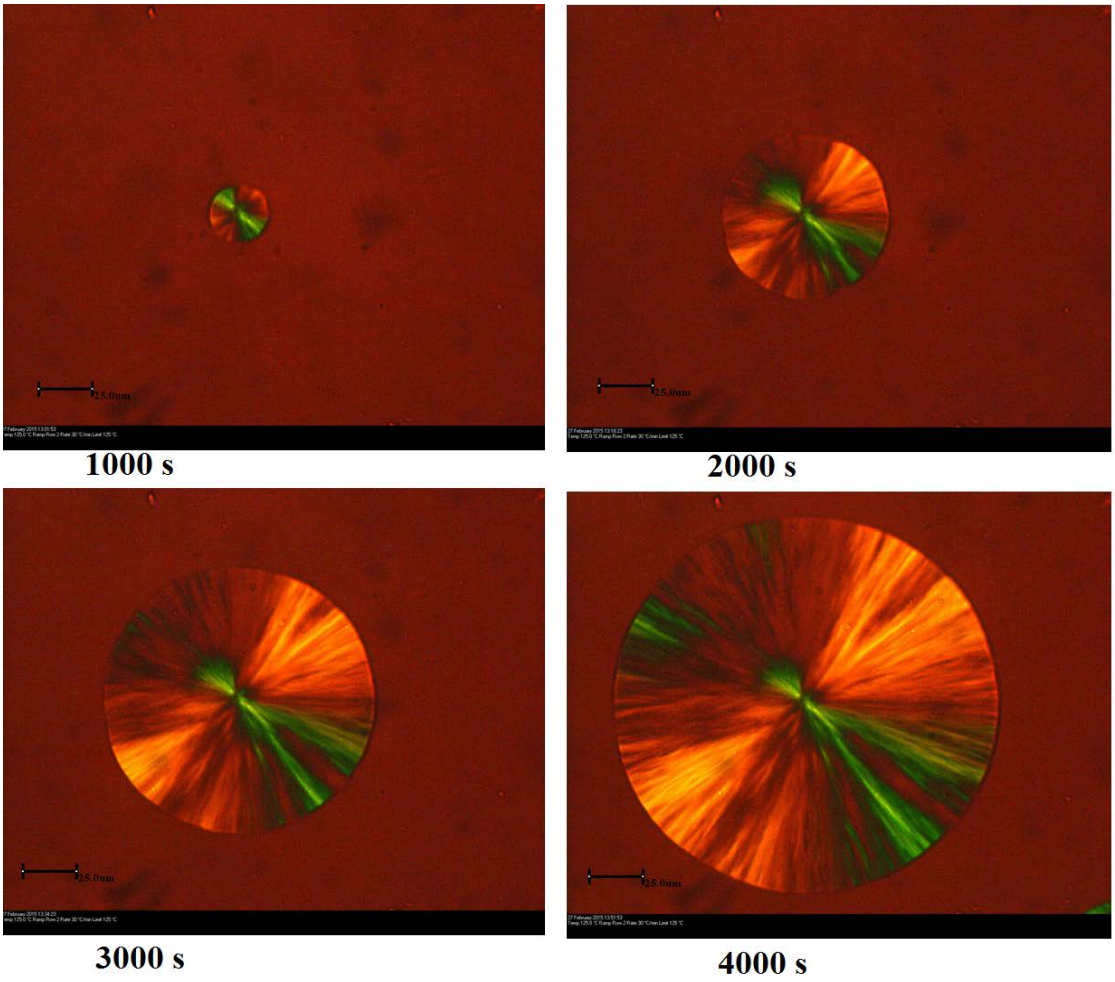

Plate 2. The Growth of a spherulite with time at 125 ^{o}C.

These conclusions were consistent with observation made on the crystallization mechanism with a light microscope. Polarized light micrographs see Plates 1 and 2 shows the growth of spherulites with time and effect of temperature on the nucleation density in thin films of co-polyLA (15 μm thick). Well-developed spherulites of similar size were observed with diameters which increased linearly with time. The spherulite growth rate, dr/dt where r is the radius of the spherulite decreased with temperature while the number was constant with time at each temperature but increased with decreasing temperature but depending on the temperature the diameter of the spherulite exceeded the film thickness early in the crystallization, see Plate 2.

The primary crystallization is attributed to heterogeneously nucleated spherulite confined to grow as discs by the thickness of the films, for which the Avrami exponent is 2.0. Studies on thicker films would be expected to yield an n value of 3.0 for growth of spheres

Secondary crystallization was observed to increase in crystallinity with the square root of the lapsed time and the rate constant increased with increasing temperature. This was consistent with diffusion controlled and attributed to the thickening of the lamellae with the square root of time leading to amorphous material trapped between the lamellae within the spherulite being converted to crystalline material. The secondary thickening of the lamellae occurs as soon as they form by the primary process and continues after the spherulites have impinged with adjacent ones. This increase in crystallinity by the secondary process is sufficient to increase the n value above that expected for the Avrami equation. The overall crystallinity, X_t, should not be used to analyze the time dependence of the overall crystallinity with the Avrami equation but only that of the primary process, $X_{p,t}$.

Eq. 9 has been derived from experimental observation and as written appears to have no limits in that X_t will tend to infinity as t tends to infinity; it should be restricted to less than 1.0 where unrealistically totally crystalline is achieved. This is not possible as there are severe restrictions on chain segments in the amorphous regions ; by geometry, chain entanglements, small segments between adjacent lamellae and near neighbor adjacent re-entry loops.

In theory, the secondary process, however, can be envisaged as having an upper limit, $X_{s,\infty}$ somewhat similar to that imposed on the primary process, $X_{p,\infty}$ such that

$$X_{p,\infty} + X_{s,\infty} \leq 1.0$$

Assuming $(X_t - X_{p,\infty} = X_{s,\infty}(1 - exp - kt^{\frac{1}{2}})$

Eqn. 9 would become

$$X_t = X_{p,\infty}[1 - \exp(-Zt^n)][1 + X_{s.\infty}\left\{1 - \exp(-kt^{\frac{1}{2}})\right\}] \qquad 9a.$$

Where k is the equivalent value for the secondary rate constant.

However, under the experimental conditions adopted the crystallinity within the spherulite boundary, as measured from the heat of fusion by DSC as a function of time [25], is low about 30-35% which means that the amorphous content is high, 60-65%. The final increased fractional crystallinity due to the secondary process is about 0.05-0.10 as shown above and well away from completion, 0.6 -0.65.

Accordingly $X_{s,\infty}(1 - exp - kt^{1/2}) \cong X_{s,\infty}\left(1 - 1 + kt^{\frac{1}{2}} - ,,,,\right) \cong X_{s.\infty}kt^{1/2}$

And with values of $X_{s,t}$ below 0.1 Eq. 9a reverts to 9 with $k_s = X_{s,\infty}k$

However there is the limit that the secondary process is limited in extent and far from reaching completion. It would be interesting to test the validity of eqn. 9 by more extended crystallizations to 10^5 or 10^6 min.

Acknowledgements

We are indebted To Mr. Frank Biddlestone for technical support.

References

[1] Hartmann MH, (1998) in DL Kaplan (Ed.), Biopolymers from renewable sources, Springer-Verlag, Berlin, pp.367-411.

[2] Dorgan JR, (1999), Poly (lactic acid) properties and prospects of an environmentally benign plastic, American Cheical Society, Washington DC, pp 145-9.

[3] Garlotta D, J. Polym and the Environment, 2001 ; **9:** 63.

[4] Kalb B, Pennings AJ, Polymer, 1980; **21: 607.**

[5] Vasanthakumari R, Pennings AJ, Polymer, 1983; **24**:175.

[6] Urbanovici E, Schneider HA, Cantow, J Polym Sci, B Polym Phys, 1984; **35**: 359.

[7] Tsuji H, Ikada Y, Polymer, 1995; **36**: 2709.

[8] Tsuji H, Ikada Y, Polymer, 1996; **37**: 595

[9] Marega C, Marigo A, DiNotto, V Zannetti R, Makromolekulare Chem, 1992; **193: 1599.**.

[10] Meaurio E, Lopez-Rodriguez N, Sarasua JR, Macromolecules 2006; **39**: 9291.

[11] Huang j, Lisowski MS, Runt JP, Hall ES, Kean RT, Buehler N, Lin JS, Macromolecules, 1998; **31**: 2593.

[12] Kolstad JJ, J Applied Polymer Sci, 1996; **62**: 1079.

[13] Krikoriam V, Pochan DJ, Macromolecules, 2005; **38**: 6520.

[14] Nomai J, Suksut B, Schlab AK, Int J App Sci Tech, 2015;8:251.

[15] Avrami MJ, J Chem Phys, 1939; **7:** 1102; 1940; **8**:212; 1941; **9** : 177.

[16] Chen Z, Hay JN, Jenkins MJ, Eur Polym J, 2016; **81**: 216.

[17] Chen Z, Hay JN, Jenkins MJ, Eur Polym J, 2013; **49**: 1722.

[18] Chen Z, Hay JN, Jenkins MJ, Eur Polym J, 2013; **49**: 2697.

[19] Phillipson K, Hay JN, Jenkins MJ, Poly Int, 2015; **64**: 1695.

[20] Phillipson K, Hay JN, Jenkins MJ, Eur Polym J, 2016; **84**: 708.

[21] Kister G, Cassanas G, Vert M, Polymer, 1998; **39**: 267.

[22] Zhang, Tsuji H, Noda I, Ozaki Y, Macromolecules, 2004; **37** : 6433.

[23] Zhang, Tsuji H, Noda I, Ozaki Y, J Chem Phys, 2004; **108** : 11514.

[24] Zhang J, Dunn Y, Sato H, Tsuji I, Noda I, Yan S, Ozaki Y, Macromolecules, 2005; **38**: 8012.

[25] Aziz AA, Ph.D Thesis, University of Birmingham, UK, 2017.